GAPFIRE MODEL DESCRIPTION

Prepared by Sam Bowers and Mathew Williams of the University of Edinburgh.

Glossary & Acronyms

AGB	Aboveground biomass, the biomass of tree stems.
Allometric equations	Tree allometry describes the quantitative relations between key, easy to measure characteristics of trees and other more difficult to assess properties. Here we relate DBH to tree morphology.
Chronosequence	A series of forest sites with similar attributes that have been regrown following clearance and abandonment, allowing the analysis of forest processes that occur over long time scales
DBH	Diameter at breast height, a measurement of tree stem size taken at 1.3 m above ground height.
Early burn	A low-intensity fire that burns early in the dry season when fuel moisture content is high. These fires are usually extinguished overnight by low temperatures and dew fall.
ECMWF	European Centre for Medium Range Weather Forecasts, source of the ERA-interim global climate reanalysis dataset.
Fire intensity	A measure of the energy released by a fire, closely related to its expected impacts upon a woodland ecosystem.
Fireline intensity	A measure of fire intensity, measured by the release of heat energy per unit time per unit length of fire front (kW/m)
FRI	Fire return interval, the mean time period between fires in years.
GapFire	The model used to predict rates of forest growth and degradation, based on the model originally published in Ryan and Williams (2011).
GPP	Gross Primary Productivity, the rate at which organisms capture and store energy through photosynthesis.
Kilwa	Miombo woodland field site in southeast Tanzania.
Late burn	A high-intensity fire that burns late in the dry season when fuel moisture content is low. These fires frequently burn through the night and are difficult to control.
MODIS	Moderate-Resolution Imaging Spectroradiometer, a NASA optical remote sensing instrument with a data archive covering the period 1999-present.
NDVI	Normalised Difference Vegetation Index, a measure of plant greenness calculated using measurements of near infrared and red spectral bands.
Nhambita	Miombo woodland field site in central Mozambique.
NPP	Net Primary Productivity, GPP minus the energy lost to respiration.
PSP	Permanent sample plot, a woodland plot used to measure and monitor vegetation status.
Top-kill	Aboveground stem mortality, which is decoupled from rootstock mortality due to the importance of resprouting in fire prone ecosystems.

1. Introduction

In order to understand the impacts of forest disturbance over long time periods, modelling techniques may be used in place of direct measurements of difficult to detect forest degradation. A dynamic model of forest biomass named GapFire has been developed to simulate the impacts of a variety of fire regimes on the structure of miombo woodlands. The model forecasts the growth and mortality of individual trees under future fire regimes based on an ensemble of tree-sized woodland patches. When run under a range of fire return intervals (FRIs) and fire intensities, the model provides a prediction of woodland response to an altered fire regime. Although a fairly simple model, GapFire has been shown to be proficient at capturing the complex dynamics of miombo woodland disturbance (Ryan and Williams, 2011).

This report provides a detailed description of how the model is structured and operated, including discussion of principal assumptions made and their impact on model predictions. Throughout the modelling process an emphasis has been placed on utilising all available field data from miombo woodlands. As data on the dynamics in some areas of miombo woodland growth, mortality and fire dynamics are limited, the model has been assembled to ensure that predictions lead to conservative estimates of biomass changes in place of a best-guess estimate of miombo woodland response.

2. Model Overview

The death of trees in natural woodlands results in small 'gaps' opening in the tree canopy. These openings in otherwise shaded forest allow for light to penetrate through the forest canopy allowing for the growth of small trees to re-populate the opening. By explicitly modelling the growth, mortality and regeneration of trees at these forest gaps, the balance between carbon sequestration through forest regrowth and carbon emission from woodland disturbance may be predicted (Figure 1). Gap dynamics are closely related to many practical forest applications, so have been widely utilised by forest land managers. Gap models are particularly appropriate for describing miombo woodlands where woodland structure is profoundly modified by frequent disturbance events. The model is similar in conception to many other gap models (Shugart and Smith, 1996, Williams, 1996) that have been used previously in miombo woodlands (Desanker, 1996, Desanker and Prentice, 1994) and also to simulate the effects of fire (Miller and Urban, 2000). A gap-modelling approach was used because of its explicit representation of population structure and variability, its ability to explore the stochastic

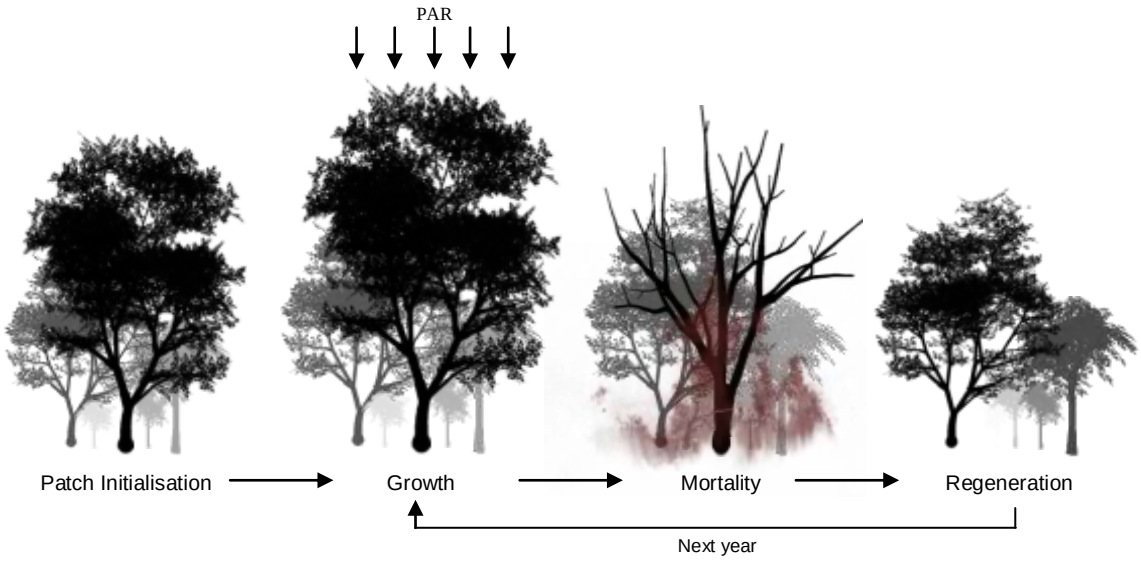

Figure 1 – Diagrammatic representation of GapFire, showing patch initialisation, growth in response to photosynthetically active radiation (PAR), fire induced mortality and regeneration.

nature of disturbance events through large modelling ensembles, and because it allowed density-dependent feedbacks on growth through light competition. The model presented here in a modified arrangement of the published model of Ryan and Williams (2011) for the prediction of biomass change.

GapFire has been constructed to model stems, their light environment, phenology, mortality and resultant carbon fluxes (Figure 2). The model simulates individual 'patches' with an area equivalent to the canopy of a large tree (0.02 ha). Light is intercepted by the leaves of each stem at a rate relating to the height of leaves in the woodland canopy. Leaf area is calculated as a function of stem diameter, and varies through the year with observations of leaf phenology, restricting growth to the wet season when soil moisture is plentiful. Intercepted light is converted to carbon using a miombo-specific light response curve. Assimilated carbon is allocated to respiration, leaf and fine-root formation, with remaining carbon allocated to increasing stem and large root biomass. As stems increase in biomass their morphology (DBH, leaf area, canopy structure) is altered according to a series of allometric models (*Appendix 1*). Following annual growth, stems are exposed to a chance of top-kill from intrinsic sources or as a result of fire, where probability of top-kill can be related to stem size, frequency and intensity of fire. Each year woodland patches regenerate, with the resprouting of top-killed rootstocks and the recruitment of new seedlings. As patches are small and mortality and regeneration processes are stochastic, the model is run as an ensemble of many patches, with the average trends relating to the net change in miombo woodland carbon storage.

The following text gives a detailed overview of initialisation, growth, mortality and regeneration in the model, which is summarised in Figure 2.

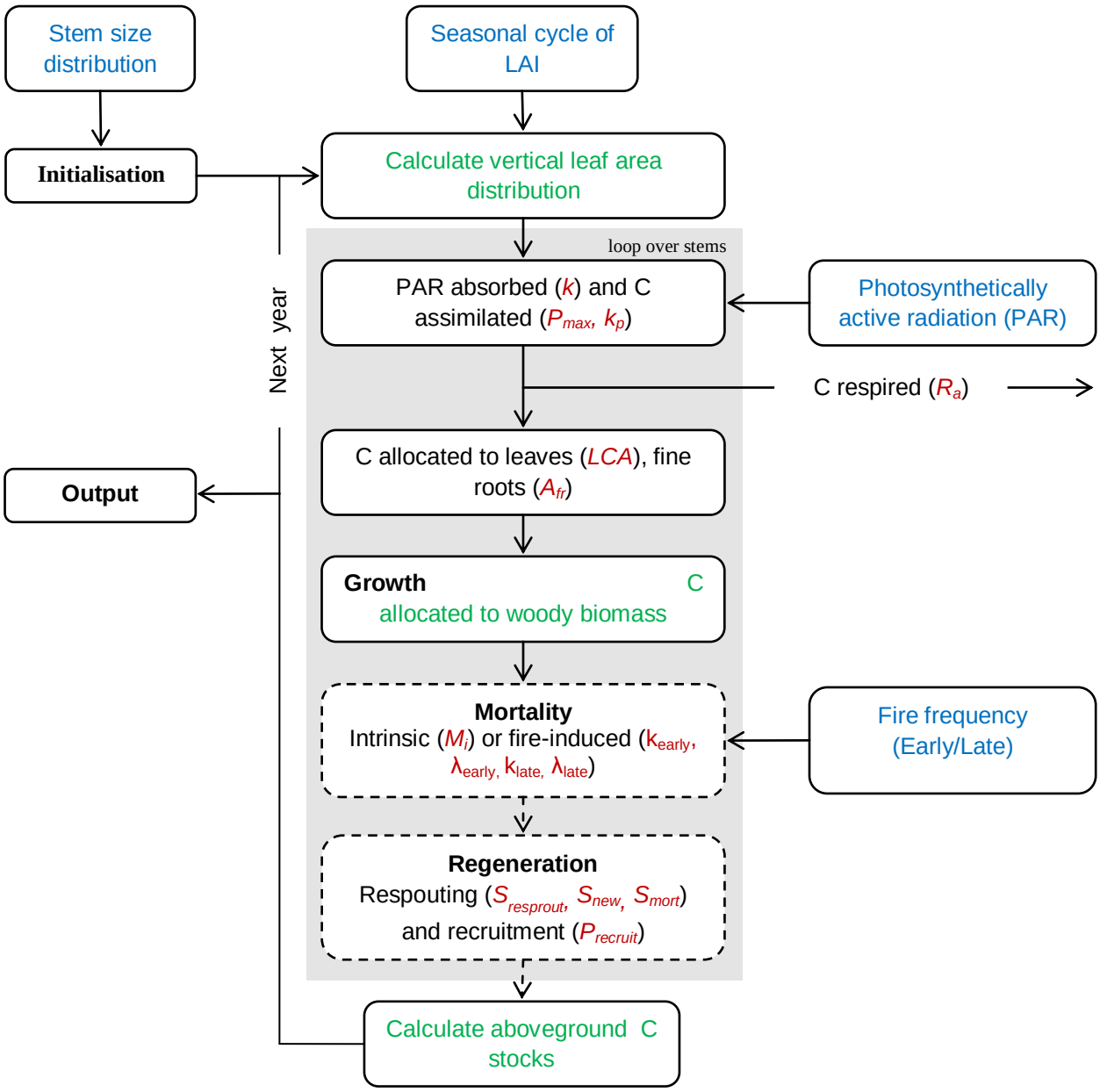

Figure 2 – GapFire model schematic. Parameters are shown in red, allometric calculations are shown in green, and model driving data is shown in blue. Stochastic processes are indicated with a dashed line. The model produces annual output, but the light and carbon assimilation functions run on hourly time steps. As patches are very small and mortality and regeneration processes are stochastic, the model runs as an ensemble of many patches.

2.1 Initialisation

Simulating characteristic conditions of miombo woodland is necessary for generating model predictions of future carbon storage. Extensive stem size data gathered from permanent sample plots (PSPs) in Kilwa are used to set up model patches with a representative stem size distribution (SSD). Of the 25 monitored PSPs, a subset of 17 were selected fitting the miombo woodland criteria (5-35 tC/ha, no closed canopy). These data comprised of a wide range of biomass measurements (5.2-33.9 tC/ha), covering 17 ha of data for stem sizes 5-40 cm DBH and 170 ha of stems >40 cm DBH. The data were fitted with two exponential trend lines, with a break point at 15 cm DBH to optimally fit observations of stem sizes (Figure 3). From these trends, two probability density functions were generated from which stem sizes may be randomly allocated to trees in model patches. A minimum stem size of 1 cm DBH was imposed to match the size that a seedling may reach following one year of growth. An upper limit of 100 cm DBH was set to prevent the generation of improbably large stems. It is assumed that the relative frequencies of stem size classes are representative of miombo woodlands as a whole and that these do not vary greatly between regions.

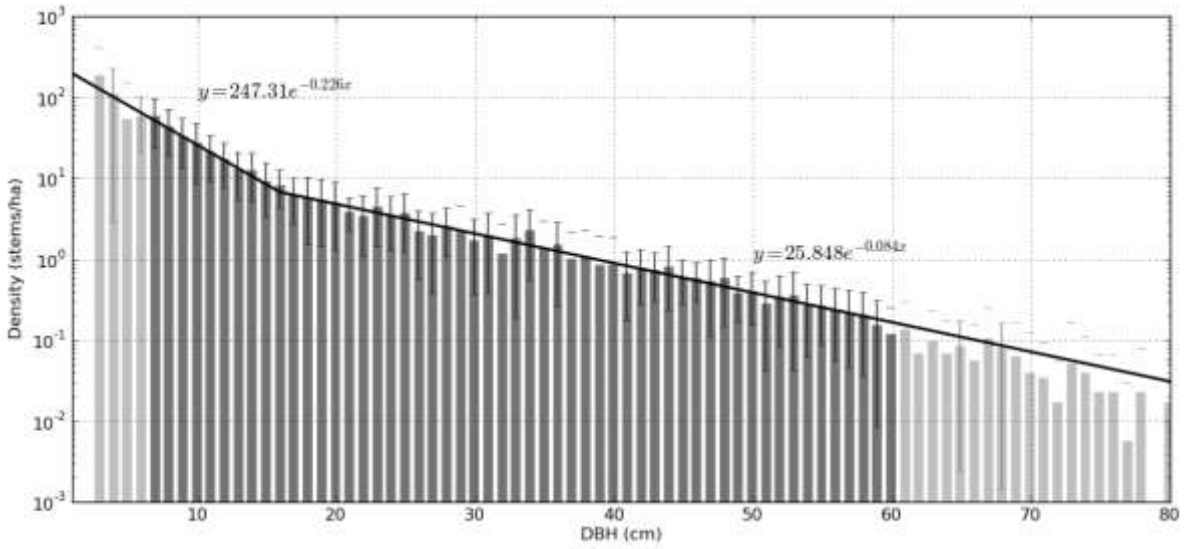

Figure 3 – Characteristic stem size distribution of a miombo woodland, fitted with trends for stems <15 cm DBH and ≥15 cm DBH. Data in light-grey were not included in trend-fitting as data for these stem sizes are limited. Data for stem sizes <5 cm DBH were not collected at the PSPs and trends are extrapolated backward. The 5-6 cm size class is also excluded as stems near the lower bound of measurement are often undercounted in sample plots. Stems >60 cm DBH are rare, so trends are extrapolated forward.

Biomass is well related to large stem density (D_{large}) (linear regression: R^2=0.668, P<0.001); accordingly the model varies large stem density to attain a range of initial biomass levels. Large stems are relatively rare (87±36 stems/ha), and occur relatively infrequently at patch-scale, therefore stems are allocated to patches based on a Poisson distribution. Little evidence was found that small stem density (D_{small}) at the PSPs varies systematically to a large degree with biomass (linear regression: R^2=0.2583, P=0.0564). Small stem density was therefore set to the mean density of 835±176 stems/ha, based on a normal distribution of stem densities. This mechanism assumes that in the 5-35 tC/ha biomass range that in miombo woodlands biomass differences are predominantly a function of large stem density.

2.2 Growth

Growth in GapFire is regulated by the light environment of each stem, which is determined from the canopy structure as determined by allometric equations (*Appendix 1*). Stem growth is further moderated by phenology, respiration and maintenance costs of trees in each patch. Growth rate is largely determined by driving data from Nhambita, and is further constrained by chronosequence data describing biomass accumulation in miombo woodlands.

2.2.1 Canopy Structure

At each patch, allometric equations are applied to relate stem DBH to tree-top and canopy base heights. Tree canopy depth (T_{depth}) is calculated as the difference of these two values, giving the vertical space amongst which each tree's leaves are distributed. A further allometric equation relates basal area of each stem to its leaf area. The canopy of each patch is represented as 25 one metre deep layers, where layers are populated with the leaf area associated with each stem, assuming that leaves are uniformly distributed in the canopy layers over T_{depth}. The total leaf area of each layer (LA_{layer}) is summed to calculate leaf area index (*LAI*):

$$LAI = \sum_{layer=1}^{25} \frac{LA_{layer}}{gap\_area} \quad (1)$$

where *gap_area* = 0.02 ha (200 m^2), approximately the area covered by the canopy of a single mature tree.

2.2.2 Light Environment

Light availability at each canopy layer is estimated using an application of the Beer-Lambert law (Jones, 1992). The Beer-Lambert law describes the attenuation of light through a tree canopy, where the top canopy layer exposed to all incoming Photosynthetically Active Respiration (*PAR*) and deeper layers are shaded by those above. PAR is absorbed according to the LA_{layer}, assuming a spherical leaf angle distribution (k = 0.5) and that all radiation is diffuse and leaves have no transmittance or albedo. Hourly estimates of *PAR* from measurements in Nhambita are used to drive photosynthesis in the model. Growth is restricted to the wet season by phenology inputs from monthly measurements of LAI in Nhambita, expressed as a fraction of peak LAI (*LAI_frac*). PAR absorbed by leaves at the top canopy layer over a year ($PAR_{maxlayer}$) is calculated from the total incoming PAR (PAR_{in}):

$$PAR_{maxlayer} = PAR_{in} \cdot \left(1 - e^{-k \cdot LA_{layer} \cdot LAI\_frac}\right) \quad (2)$$

PAR transmitted through to lower layers (PAR_{thru}) is calculated by differencing PAR_{in} and $PAR_{maxlayer}$.

$$PAR_{thru} = PAR_{in} - PAR_{maxlayer} \quad (3)$$

Light absorption at further layers (PAR_{layer}) is calculated down through the further 24 canopy layers:

$$PAR_{layer} = PAR_{thru} \cdot \left(1 - e^{-k \cdot LA_{layer} \cdot LAI_{frac}}\right) \quad (4)$$

$$PAR_{thru} = PAR_{layer+1} - PAR_{layer} \quad (5)$$

This produces a vertical profile of light absorption in each patch through each year, which drives the photosynthesis and growth of each stem.

2.2.3 Carbon Assimilation

Growth is determined separately for each stem, with absorbed PAR converted to assimilated carbon using photosynthetic light response curves. Two parameters describe the light response curve: the maximum rate of assimilation (P_{max}) and the amount of light needed to achieve half this rate (k_p). For each stem, mass of photosynthate is summed for each canopy layer for each hour of the 12 diurnal cycles representative of each month, and scaled up to a yearly total. The gross primary productivity of each stem at each layer for each hour of daylight (GPP_i) is calculated as a proportion of maximum photosynthetic rate (P_{max}) and the total leaf area of each tree (LA_{tree}):

$$GPP_i = \left[P_{max} \cdot \frac{PAR_{layer}}{PAR_{layer} + k_p} \cdot LAI\_frac\right] \cdot LA_{tree} \quad (6)$$

The sum of GPP_i over all layers over the entire year gives the total carbon fixation by each tree from photosynthesis (*GPP*). Net primary productivity of each stem (*NPP*) is calculated as GPP minus the fraction of carbon that is respired by the plant (R_a):

$$NPP = GPP \cdot (1 - R_a) \quad (7)$$

Carbon required for the yearly replacement of leaves (C_{leaf}) is calculated as a function of leaf carbon per unit area (*LCA*) and the total tree leaf area (LA_{tree}):

$$C_{leaf} = LA_{tree} \cdot LCA \quad (8)$$

C_{leaf} and fine root carbon (C_{fr}) are deducted from NPP, leaving carbon allocated to woody biomass (C_{wood}).

$$C_{wood} = NPP - C_{leaf} - C_{fr} \quad (9)$$

Carbon allocation for each tree is partitioned to above and below ground pools in proportion *shoot_frac*, following an allometric relationship. Stem carbon allocation (C_{stem}) can therefore be calculated as:

$$C_{stem} = shoot\_frac \cdot C_{wood} \quad (10)$$

Stem growth is calculated as the annual increase in C_{stem}, which is related to an equivalent increase in DBH by an allometric model. This series of calculations accounting for growth are repeated for each stem, producing a yearly estimate of growth in each woodland gap.

2.3 Mortality

GapFire models stem mortality in response to fire occurrence and intrinsic (non-fire) sources. Because of the importance of resprouting in fire-prone ecosystems (Bond and Midgley, 2001, Chidumayo, 2004, Mlambo and Mapaure, 2006), aboveground stem mortality (top-kill) was decoupled from belowground rootstock mortality. The mortality module accounts for stem top-kill, whereas rootstock mortality is calculated with plot regeneration. Fires are stratified into early burns and late burns, which occur with probability *P(early)* and *P(late)*.

2.3.1 Fire-induced Top-kill

Stems are top-killed each year by either intrinsic sources, such as senescence, herbivory, elephant damage and timber extraction, or as a result of fire. In a year that fire does not occur, intrinsic mortality probability (M_i) is set at a constant rate for all size classes. In the case of fire, stem top-kill rates are derived from field experiments in Mozambique, which showed stem top-kill to be a function of stem diameter and thermal anomaly (Ryan and Williams, 2011). As stem diameter increases, thickness of protective bark increases proportionally (Jackson et al., 1999, Sutherland and Smith, 2000, Johnson and Miyanishi, 2001), offering greater resilience as trees increase in size. In larger stems (>10 cm DBH), this effect saturates, and further increases in DBH provide no additional protection from fire. This relationship was modelled with a sigmoidal function, with saturation for larger stems:

$$log\ odds\ of\ top\text{-}kill = -a_x DBH + b_x \quad \text{where DBH}<10\text{cm} \tag{11}$$

$$log\ odds\ of\ top\text{-}kill = b_{x\_sat} DBH \quad \text{where DBH}>10\text{cm} \tag{12}$$

Variables a_x, b_x, and b_{x_sat} are determined by fire intensity. A continuous relationship between fire intensity and mortality parameters is determined from measurements of stem mortality and fireline intensity (*FLI*) from the Nhambita fire experiments (Saito et al., *in prep*). FLI is defined as the release of heat energy per unit time per unit length of fire front (kW/m) (Byram, 1959). It is widely utilised because it is relatively easy to measure, and it is known to be significantly correlated to biologically important fire impacts including tree top-kill and mortality (Alexander, 1982). Fireline intensity is calculated as:

$$FLI = H \cdot w \cdot R \tag{13}$$

where H = heat yield (kJ/kg), w = mass of available fuel (kg) and R = rate of spread of fire front (m/s). Its relationship to top-kill variables was determined to be:

$$a_x = -7.025 \cdot \ln(FLI) - 13.112 \tag{14}$$

$$b_x = 2.119 \cdot \ln(FLI) - 12.451 \tag{15}$$

$$b_{x\_sat} = -123.5 \cdot FLI^{-0.498} \tag{16}$$

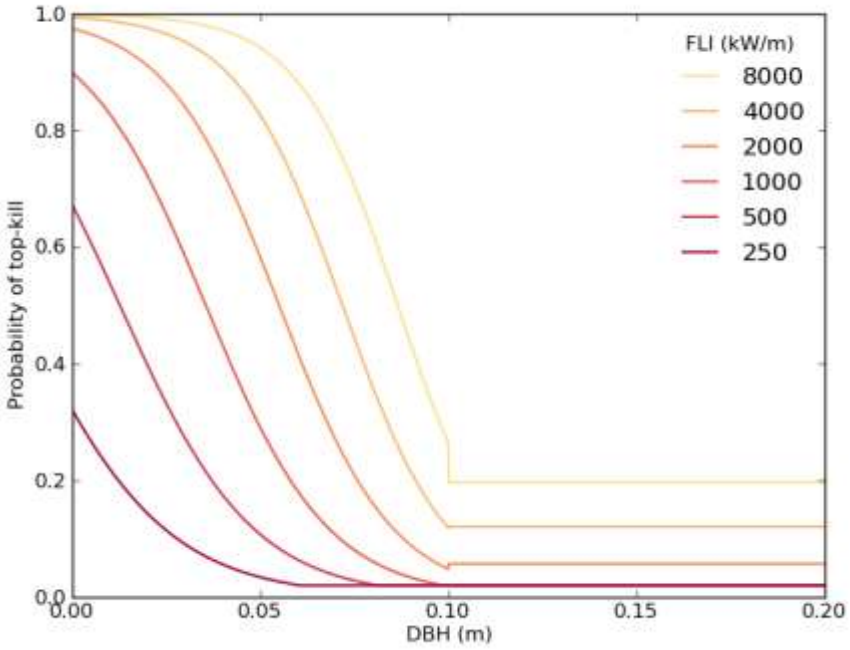

Figure 4 – Fire-induced stem top-kill rates with stem DBH and fireline intensity (FLI).

A minimum mortality rate is set to the value of M_i for all fire intensities. This results in a continuous relationship between fire intensity and top-kill (Figure 4).

2.3.2 Fire Seasonality

It is widely recognised that low intensity early-season fires are much less damaging than high intensity late-season fires (Campbell, 1996, Hoffa et al., 1999, Goldammer and De Ronde, 2004, Robertson, 1993). GapFire stratifies fires into early and late categories, each with a characteristic range of intensities. Fire intensity is described by two Weibull distributions, defined by parameters k_{early}, λ_{early}, k_{late}, λ_{late}, from which a fireline intensity is randomly allocated to each early/late fire. These two distributions incorporate the variability of fire intensity that is expected of wildfires and the differences between average early and late fire intensity.

2.3.3 Fire Frequency

P(early) and *P(late)* are input as a model drivers. For further information on their generation, refer to report from University College London.

2.4 Regeneration

Top-killed stems above a minimum size class ($S_{resprout}$) when killed have a probability of resprouting (*1* - S_{mort}), where S_{mort} is probability of rootstock mortality based on data from the Nhambita fire experiments. It is assumed that sprouts reach 2cm DBH in their first year of growth. Additionally there is a chance of a recruitment event occurring ($P_{recruit}$), where a number of new seedlings (S_{new}) are established in a patch, reaching 1cm DBH in their first year of growth. The initial growth of seedlings is assumed to be smaller than sprouts due to the established sprout rootstocks providing energy for increased growth.

2.5 Output

Following the growth, mortality and regeneration at each patch at each year, carbon stocks are summed using the allometric relation between stem DBH and aboveground biomass. The model only includes stems of >5 cm DBH when calculating biomass due to uncertainties in the dynamics of small stems and to match measurement protocols a the Kilwa PSPs. Allometric models are also used produce estimates of LAI and rootstock biomass, which in conjunction with basal area and stocking density counts are used as model validation. As each forest patch is very small and fire and regeneration occur stochastically, the biomass change in a single patch will not represent the trends of miombo woodland as a whole. The model is therefore run as an ensemble, where the biomass trend is taken to be the average biomass trend from a large number of patches.

Table 1 – Model parameter values, their source, nominal values and sensitivity S_x. Sensitivity analysis was conducted on an ensemble of 5000 patches under an intense fire regime (FRI = 1.11, p(burn|early)=0.33, p(burn|late)=0.66) and in the absence of fire, with the response variable set as 10-year change in aboveground biomass of an average biomass (21 $tC \cdot ha^{-1}$) woodland. Model sensitivity is defined as $S_x = ([R_{adj} - R_n]/ R_n) / ([P_{adj} - P_n]/ P_n)$, where x is the factor by which the nominal value is changed, R_{adj} is the response for the model run with the adjusted value, R_n is the response with the nominal value, and P_n and P*adj* are the parameter values for the nominal and adjusted cases respectively.

			Intense Fire				No Fire				
Parameter description	**Parameter name**	**Nominal parameter value, P_n**	**$S_{0.5}$**	**$S_{0.75}$**	**$S_{1.5}$**	**S_2**	**$S_{0.5}$**	**$S_{0.75}$**	**$S_{1.5}$**	**S_2**	**Source of nominal parameter value**
Growth Parameters											
Fraction of GPP used for autotrophic respiration	R_a	0.5	4.5	3.6	3.2	1.8	-3.6	-3.4	-2.6	-1.5	(Waring et al., 1998)
Extinction coefficient for Beer-Lambert law	k	0.5	-0.1	-0.6	0.0	0.0	-0.1	-0.2	0.0	0.0	(Norman and Campbell, 1991)
Amount of C allocated to fine roots, as a fraction of allocation to leaves	C_{fr}	1	0.8	0.3	1.0	0.7	-0.8	-0.7	-0.6	-0.6	(Hendricks et al., 2006, Castellanos et al., 2001)
Maximum rate of photosynthesis ($\mu molC \cdot m^{-2} \cdot s^{-1}$)	P_{max}	12	-3.1	-3.4	-4.3	-4.8	2.6	2.8	3.7	4.3	(Tuohy and Choinski, 1990, Tuohy et al., 1991, Woollen, 2013)
PAR intensity at which 0.5*Pmax* is obtained ($\mu mol \cdot s^{-1} \cdot m^{-2}$)	k_p	250	3.1	1.9	1.5	1.1	-2.7	-2.1	-1.1	-0.9	(Tuohy and Choinski, 1990, Tuohy et al., 1991, Woollen, 2013)
Leaf carbon per leaf area ($gC \cdot m^{-2}$)	LCA	50	1.6	1.3	1.6	1.3	-1.4	-1.4	-1.2	-1.1	(Nottingham, 2004, Chidumayo, 1997)
Mortality & Regeneration Parameters											
Intrinsic mortality rate	M_i	0.02	0.2	-0.1	0.4	0.4	-0.8	-0.9	-0.7	-0.7	Estimated (Ryan and Williams, 2011), similar to Desanker & Prentice (1994)
Early burn intensity scale	k_{early}	1065	0.2	0.1	0.5	0.4	-	-	-	-	Rothermel model, similar to Hoffa et al. (1999), Robertson (1993)
Early burn intensity shape	λ_{early}	1.86	-0.5	-0.4	0.0	-0.1	-	-	-	-	Rothermel model, similar to Hoffa et al. (1999), Robertson (1993))
Late burn intensity scale	k_{late}	3498	3.3	2.7	2.0	1.7	-	-	-	-	Rothermel model, similar to Ryan & Williams (2011), Shea et al. (1996)
Late burn intensity shape	λ_{late}	2.78	0.2	-0.3	0.5	0.2	-	-	-	-	Rothermel model, similar to Ryan & Williams (2011), Shea et al. (1996)
DBH at which seedling develops rootstock and the ability to resprout (m)	$S_{resprout}$	0.02	0.1	-0.4	0.1	0.0	-0.1	0.0	0.1	0.0	Estimated (Ryan and Williams, 2011)
Number of seedlings established in a recruitment year (ha^{-1})	S_{new}	5000	-0.2	0.2	0.2	0.0	0.0	-0.1	0.0	0.0	Estimated (Ryan and Williams, 2011)
Probability of a recruitment year occurring	$P_{recruit}$	0.03	-0.1	-0.5	0.2	0.2	-0.1	-0.1	0.1	0.0	Estimated (Ryan and Williams, 2011)
Probability of a rootstock failing to resprout following fire	S_{mort}	0.04	-0.1	-0.8	0.0	0.1	0.0	0.1	0.0	0.0	(Ryan and Williams, 2011)

3. Parameter Estimation and Model Sensitivity

Parameter values were derived from the literature, field measurements and assessed with reference to local knowledge. All parameters are unchanged from the originally published model, with the exception of maximum photosynthetic rate (P_{max}). Model sensitivity was evaluated with respect to changes to nominal parameter values (Table 1). Where the model is found to be sensitive to a parameter change, an assessment is made about how well constrained the parameter is by available data. Model parameters are considered in two categories: parameters determining growth and those controlling mortality and regeneration.

3.1 Growth Parameters

Of the parameters controlling patch growth, model predictions were found to be sensitive to respiratory fraction (Ra), maximum photosynthetic rate (Pmax) and half saturation of photosynthetic rate (kp). These three parameters relate to the productivity of miombo woodlands by controlling carbon assimilation and growth rate. Respiratory fraction determines the proportion of carbon assimilated through photosynthesis that is lost to the atmosphere through plant respiration. Respiratory fraction is poorly constrained within savannah woodlands, as it is very difficult to measure in situ. However, it is well constrained globally at around 50% (Waring et al., 1998). A significant deviation from this value in miombo woodlands is not expected. Maximum photosynthetic rate and half saturation describe the rate of photosynthesis that is expected under different light conditions. Maximum rate of photosynthesis occurs under optimal light conditions, and this value likely to lie in the range 9-15 µmolC·m-2·s-1 (Tuohy and Choinski, 1990, Tuohy et al., 1991, Woollen, 2013). Though individual parameter values determining miombo woodland growth are uncertain, there are good data on miombo regrowth following woodland clearance which can demonstrate that growth in the absence of fire is represented appropriately by the model (see section 4.1).

Table 2 - Observations of fire behaviour in Southern African savannah and miombo woodland vegetation. *Acknowledgement: Bill Higham*.

Fuel Type	**Location**	**ROS** (m/min)	**Flame Length** (m)	**Intensity** (kW/m)	**Source**
Miombo	Mozambique	3 - 55		360 - 6600	(Ryan and Williams, 2011)
Savannah	South Africa	0.6 - 102		28 - 17905	(Govender et al., 2006)
Savannah	Zambia	1.2 - 105.6	0.3 - 4.2	43 - 9476	(Hély et al., 2003)
Miombo	Zambia	6 - 48	0.7 – 3.2	25 - 6553	(Hoffa et al., 1999)
Savannah	South Africa	12 - 60	1 - 6	475 - 6130	(Shea et al., 1996)
Miombo	Zambia	18 - 48	3 - 5	1734 - 4061	(Shea et al., 1996)
Savannah	South Africa				
	Block 55	97.2	3.5	10906	(Stocks et al., 1996)
	Block 56	37.8	1.7	4048	
Savannah	South Africa		0.5 - 6		
	Head	4.2 - 28.8		93 - 3644	(Trollope et al., 1996)
	Back	0.0 - 15		20 - 160	
Miombo	Zimbabwe				
	Early			100 - 300	(Robertson, 1993)
	Late			500 - 5000	

3.2 Mortality & Regeneration Parameters

AGB change was found to be largely insensitive to parameters controlling miombo regeneration. Over the time-scales of a REDD+ project, mechanisms of regeneration are not expected to be hugely important as biomass change is concentrated in large stems which regenerate over several decades. Over longer timescales it is expected that fire will reduce pressure on seedlings and sprouts by exposing stems to lower intensity and less frequent fires. The lifting of this 'demographic bottleneck' should improve the capacity of woodlands to regenerate, though the impacts of these changes may only be observable in the decades following fire management.

Stem mortality is considerably greater importance to model output, particularly fire-induced top-kill. This signals the importance of fire to the productivity of miombo woodlands. Fire seasonality is approximated by a modelling approach combined with a thorough review of literature on African savannah fires. Data on fire behaviour in miombo woodlands is scarce, though there is much information on fire behaviour in savannah grasslands, particularly from South Africa (Table 2). Fire intensity in miombo woodlands varies from very low (<300 kW/m) to high intensity (>6500 kW/m). There is also the potential for extremely high intensity fires (>10000 kW/m), though these have not been measured in miombo woodlands by fire experiments. Of particular significance are the results of Hoffa et al. (1999), where a series of early-season fires were measured that showed a progression from very low intensities through to the higher intensities observed by the mid dry season (Figure 5). Robertson (1993) also recorded the differences between early and late burns, measuring early burns to be of very low intensity (<300 kW/m) and late burns to be considerably more intense and more variable (500-5000 kW/m). Ryan and Williams (2011) set fires at different times of day and exploited within fire variability to achieve a wide range of fire intensities when burning in the late dry season. Fires early in the morning were of similar intensity to early burns (360 kW/m), with the highest intensities reaching 6600 kW/m at the hottest part of the day. Though currently available literature cannot provide all the required detail about seasonal variability in fire intensity, it does give a suitable envelope of probable fire intensities in miombo woodlands.

Further descriptors of fire seasonality may be generated using widely-used models of fire intensity. The Rothermel model is a semi-empirical model of fire spread that has been widely used to understand variation in fire intensity in a wide range of fire systems (Rothermel, 1972). Its equations lie at the centre of many modern fire models, including the United States Department of Agriculture system for the evaluation of operational fire hazard (Pyne et al., 1996) and in the SPITFIRE module to the LPJ dynamic global vegetation model (Thonicke et al., 2010). Its modest input requirements and adaptability make it an appropriate means of approximating seasonal fire intensity variation in miombo woodlands. The Rothermel model was parameterised using values from the literature as well as field data from Kilwa, and driven by meteorological data from the ECMWF ERA-interim climate reanalysis dataset and fuel curing estimates generated from the MODIS archive. The model arrangement is described in *Appendix 2*. The Rothermel output was used to generate distributions describing the intensity of early and late burns (Figure 6). Based on driving data from 2000-2012 and an early/late cut-off date of the end of June, two Weibull distributions were fitted that qualitatively fit expected fire intensities, with good matches for the expected seasonal fire intensity range.

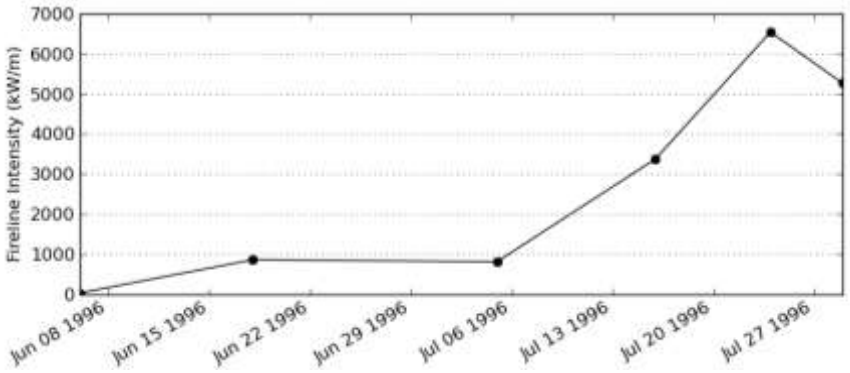

Figure 5 – Fire intensity measurements in Zambia from Hoffa et al. (1999), showing a trend of increasing intensity through the fire season.

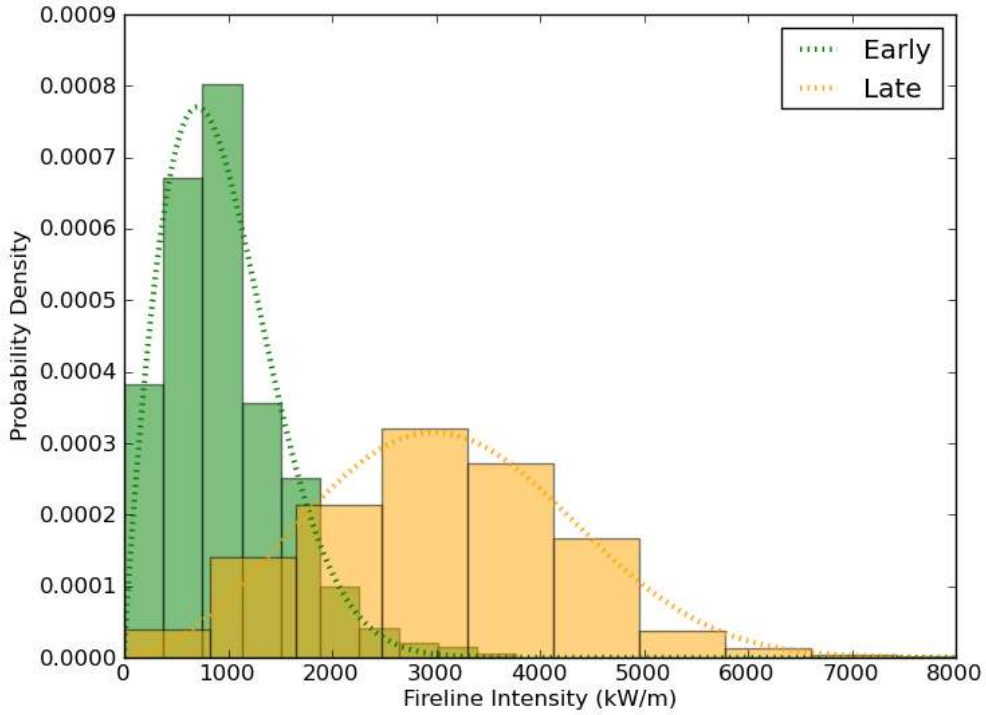

Figure 6 – Normalised histograms of early and late fire intensities predicted by the Rothermel model, fitted with Weibull distributions. Distributions are defined by scale (k) and shape (λ_{early}) parameters, with values of k_{early} = 1065, k_{late} = 1.86, λ_{early} = 3498 and λ_{late} = 2.78.

4. Model Evaluation

4.1 Patch Growth

Assumptions relating to growth parameters were validated using chronosequence field data from Nhambita. A chronosequence is a series of forest sites with similar attributes that have been regrown following clearance and abandonment, allowing the analysis of forest processes that occur over long time scales, in this case forest regrowth. The chronosequence predicts approximately 0.7 tC/ha to be assimilated each year on abandoned land which has not been observed to burn. This situation was simulated by running the model from a start-point with no large stems through 25 years in the absence of fire (Figure 7).

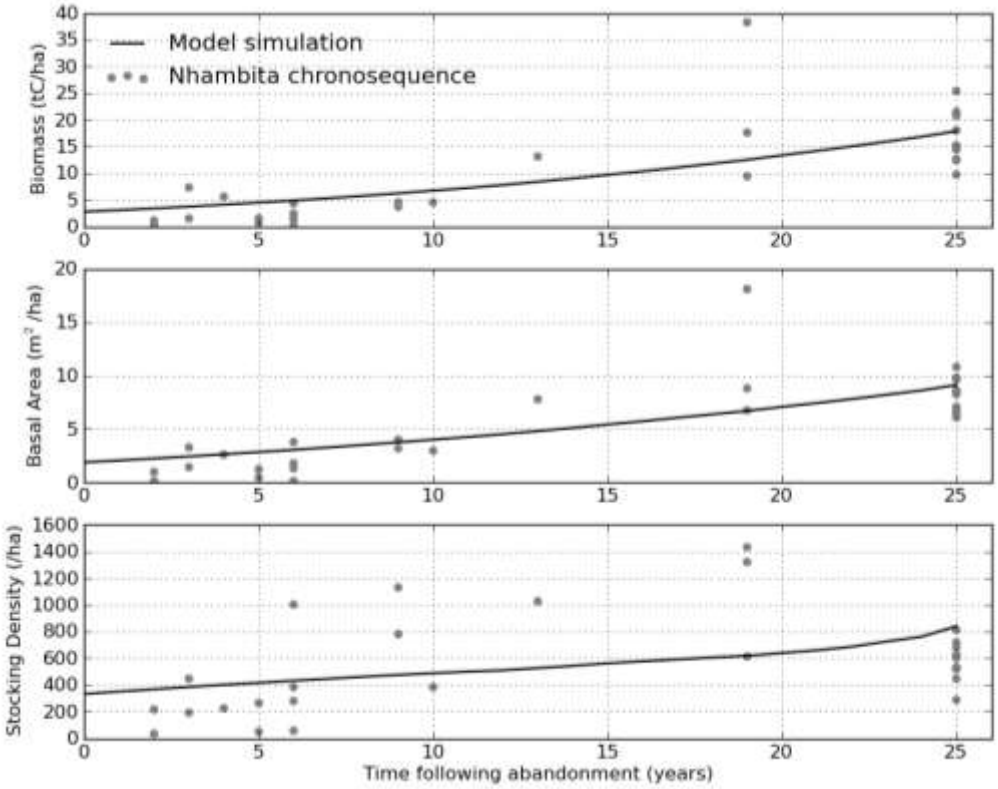

Figure 7 – Model output comparison to chronosequence data from Nhambita. Biomass increase following abandonment is predicted accurately (RMSE = 5.3 tC/ha, R^2=0.66), as is basal area (RMSE = 1.7 m^2/ha, R^2=0.84), though the model is not able to very effectively capture trends stocking density of trees >5 cm DBH (RMSE = 250 ha^{-1}, R^2=0.53).

The model suggests a sigmoidal growth form, relating to exponentially increasing stand productivity with biomass up to a saturation point. Average growth rates over 25 years amount to a biomass increment of 0.63 tC/ha, a level slightly lower than observed in the chronosequence. The model predicts basal area appropriately, with growth rate matching observations. The model is less able to predict stocking density, likely due to the initialisation of 'bare' patches with a stock of saplings, highlighting a limitation in the model representation of regeneration. This data represents a conservative estimate of miombo woodland productivity as the annual biomass increase is below that observed. Additionally, chronosequence observations are assumed to be in the total absence of fire, something which is unlikely to be the case.

4.2 Fire Intensity

It is not possible to fully evaluate the Rothermel model due to the lack of appropriate validation data from miombo woodlands. However, we are able to demonstrate that the predicted intensities for early and late fires are reasonable, and thus result in a conservative rate of stem top-kill. The review of the literature on miombo fires suggests that early burns have an intensity of less than 500 kW/m, whereas the Rothermel model predicts fire intensity to frequently rise above 1000 kW/m. Late season fires have a very large range of intensities, from 500 kW/m to over 6000 kW/m, averaging around 4000 kW/m. The Rothermel model predicts a median late fire intensity of around 3000 kW/m, and that fire intensity rarely rises above 6000 kW/m. For the requirements of a REDD+ project, this is appropriate as it will lead to a conservative estimate of the efficacy of early burning and the rate of forest degradation in the baseline scenario, provided that during the project early burn frequency increases and late burn frequency decreases. The Rothermel model estimate of fire intensity is based upon a fixed early/late cut-off date of the end of June. In reality, climatic variability will shift this date annually, so with careful observation it can be ensured that prescribed burns will always be at the lower end of the intensity range.

5. Using the Model

The model has been ported into Microsoft Excel as a familiar environment for users to examine detailed model outputs. The spreadsheet provided does not contain any of the model itself, but is an interface for setting model parameters and visualising outputs. The spreadsheet allows for simple use of commonly used model functions, and also analysis of the impact of parameter changes and the exploration of raw data outputs. Here we describe use of the model for prediction of carbon storage changes from a modified fire regime.

The model is provided in a compressed folder ('GapFire.zip'), and should be unzipped to the C:\ drive. Open 'GapFire.xlsm' to access the model spreadsheet, ensuring to dismiss the security warning that appears at the top of the workbook ('Enable Content'). The primary controls for the model are number of ensembles ('patches'), initial biomass, and frequency of early and late fires in the baseline and project scenarios (Figure 8). Increasing the number of patches will result in a less variable output, but will increase model run time. A minimum of 10,000 patches should be used to achieve a reliable model run, with 100,000 patches recommended if time is available. Initial biomass can be altered to reflect the mean starting biomass of patches. Due to the random allocation of stems to each patch the actual initial biomass may be slightly different to that selected. Fire frequency should be input based on historical fire mapping and ongoing monitoring. Note that the probability of no fire is equal to *1 – pEarly – pLate*.

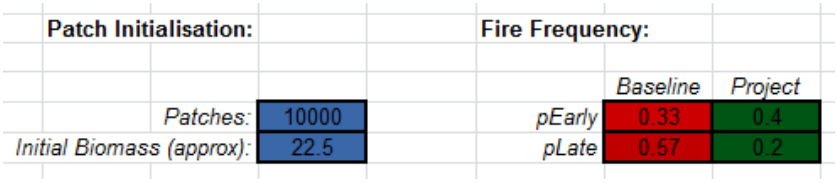

Figure 8 – Primary inputs to the model for use in carbon accounting.

To run the model, the parameter input file should first be updated using 'Update Parameters', which writes selected parameters to a comma separated variables (.csv) file. The model is started using 'Run GapFire' and once complete the spreadsheet should be updated with new model outputs using 'Update Results' (Figure 9).

Figure 9 – Model controls, initiating 1) writing of model input file, 2) model run, and 3) spreadsheet update.

Model outputs are summarised in a table showing aboveground carbon storage in the baseline and project scenarios, along with estimates of avoided emissions, sequestered carbon and net change (Figure 10). This summary contains the information required for a REDD+ project to audit carbon storage.

Output Summary:

Tonnes C / hectare

Years	*Baseline*	*Project*	*Avoided Emissions*	*Sequestered Carbon*	*Change*
0	22.59	22.59	0.00	0.00	0.00
5	20.25	23.46	2.34	0.87	3.21
10	18.36	24.40	4.23	1.82	6.04
20	15.06	25.63	7.52	3.05	10.57
50	7.01	25.68	15.57	3.09	18.66

Figure 10 – Summary of carbon storage change predicted by the model.

A graphical summary of carbon storage change in the project and baseline scenarios is also generated, as well as estimates of carbon storage change between the two scenarios and the rate of carbon accumulation (Figure 11). This data is also presented in a raw format to allow for more detailed analysis of potential project impacts.

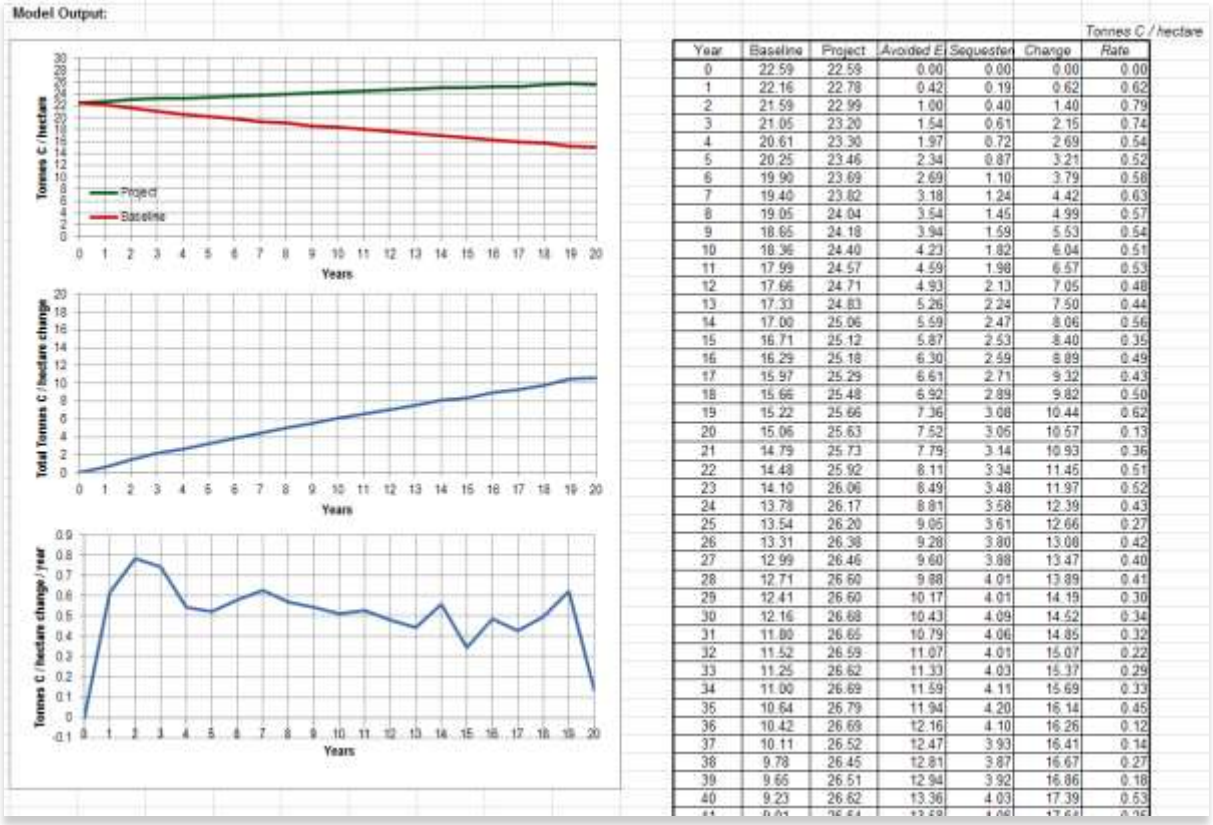

Year	Baseline	Project	Avoided E	Sequester	Change	Rate
0	22.59	22.59	0.00	0.00	0.00	0.00
1	22.16	22.78	0.42	0.19	0.62	0.62
2	21.59	22.99	1.00	0.40	1.40	0.79
3	21.05	23.20	1.54	0.61	2.15	0.74
4	20.61	23.30	1.97	0.72	2.69	0.54
5	20.25	23.46	2.34	0.87	3.21	0.52
6	19.90	23.69	2.69	1.10	3.79	0.58
7	19.40	23.82	3.18	1.24	4.42	0.63
8	19.05	24.04	3.54	1.45	4.99	0.57
9	18.65	24.18	3.94	1.59	5.53	0.54
10	18.36	24.40	4.23	1.82	6.04	0.51
11	17.99	24.57	4.59	1.98	6.57	0.53
12	17.66	24.71	4.93	2.13	7.05	0.48
13	17.33	24.83	5.26	2.24	7.50	0.44
14	17.00	25.06	5.59	2.47	8.06	0.56
15	16.71	25.12	5.87	2.53	8.40	0.35
16	16.29	25.18	6.30	2.59	8.89	0.49
17	15.97	25.29	6.61	2.71	9.32	0.43
18	15.66	25.48	6.92	2.89	9.82	0.50
19	15.22	25.66	7.36	3.08	10.44	0.62
20	15.06	25.63	7.52	3.05	10.57	0.13
21	14.79	25.73	7.79	3.14	10.93	0.36
22	14.48	25.92	8.11	3.34	11.45	0.51
23	14.10	26.06	8.49	3.48	11.97	0.52
24	13.78	26.17	8.81	3.58	12.39	0.43
25	13.54	26.20	9.05	3.61	12.66	0.27
26	13.31	26.38	9.28	3.80	13.08	0.42
27	12.99	26.46	9.60	3.88	13.47	0.40
28	12.71	26.60	9.88	4.01	13.89	0.41
29	12.41	26.60	10.17	4.01	14.19	0.30
30	12.16	26.68	10.43	4.09	14.52	0.34
31	11.80	26.65	10.79	4.06	14.85	0.32
32	11.52	26.59	11.07	4.01	15.07	0.22
33	11.25	26.62	11.33	4.03	15.37	0.29
34	11.00	26.69	11.59	4.11	15.69	0.33
35	10.64	26.79	11.94	4.20	16.14	0.45
36	10.42	26.69	12.16	4.10	16.26	0.12
37	10.11	26.52	12.47	3.93	16.41	0.14
38	9.78	26.45	12.81	3.87	16.67	0.27
39	9.65	26.51	12.94	3.92	16.86	0.18
40	9.23	26.62	13.36	4.03	17.39	0.53

Figure 11 – Model output graphical and tabular summary.

Further information is presented on the ‘Parameters’ worksheet, where model parameters and variables can be altered. Raw model outputs are displayed in the ‘DATA’ worksheet, where additional model outputs can be explored.

Appendix 1: Allometric Equations

Tree allometry describes the quantitative relations between key, easy to measure characteristics of trees and other more difficult to assess properties. Allometric relationships derived from destructive measurements of trees in miombo woodland in Nhambita are used extensively in the model. The allometric models used are summarised in Table 3, and their derivation described in detail in Ryan et al. (2011).

Table 3 – Allometric equations used in the model, derived from miombo woodland data in Nhambita. Equation forms are defined as: Power, $y = ax^b$, Linear, $y = ax+b$. n is the number of samples used to fit the function, and R^2 gives the proportion of variance described by the allometric model.

Dependent (y) variable	Independent (x) variable	Form	a	b	n	R^2	notes
C stock of stem (kg C)	DBH (m)	Power	4222	2.6	29	0.93	
C stem : C root+stem	DBH (m)	Linear	0.32	0.6	23	0.26	
Height of tree top (m)	DBH (m)	Linear, with saturation	42.6		80	0.67	where DBH >60cm , height = 25 m
Height of canopy base (m)	DBH (m)	Linear, with saturation	22.3		80	0.58	where DBH >67 cm, canopy base = 15 m.
Leaf area (m)	Basal Area (m^2)	Linear	1330		10	0.29	Plot-scale data

Appendix 2: The Rothermel Model

Rothermel's model simulates fire as a quasi-steady state series of ignitions in a spatially uniform fuelbed. Rate of fire spread is modelled as the ratio of propagating heat flux to the energy required to dry out and ignite unburned fuels. Fire rate of spread is influenced by the geometry, composition and moisture content of the fuelbed, and multiplicative factors describing wind speed and slope. The complete Rothermel model of fire spread is:

$$R = \frac{I_R \xi (1 + \phi_w + \phi_s)}{\rho_b \varepsilon Q_{ig}} \quad (17)$$

where R = rate of spread (m min^{-1}), I_R = reaction intensity of the flaming front (kJ m^{-2} min^{-1}), ξ = propagating flux ratio (dimensionless), φ_w = wind coefficient (dimensionless), φ_w = slope coefficient (dimensionless), ρ_B = fuelbed bulk density (kg m^{-3}), ε = effective heating number (proportion of fuel raised to ignition temperature) (dimensionless), and Q_{ig} = heat of pre-ignition (quantity of heat required to ignite fuel, a function of moisture content) (kJ kg^{-1}). Reaction intensity (I_R) is the product of several factors that relate to rate of energy release, defined by:

$$I_R = \Gamma' W_n h \eta_M \eta_s \quad (18)$$

where Γ' = optimum reaction velocity (min^{-1}), W_n = net fuel loading (kg m^{-2}), h = low heat content (kJ kg^{-1}), η_M = moisture damping coefficient and η_s = mineral damping coefficient. Reaction velocity is calculated as a function of surface area to volume ratio (σ). For further information on the formulation of the Rothermel model, refer to Rothermel (1972). Importantly, the Rothermel model can be applied to estimate of fireline intensity by combining modelled rate of spread with combustion completeness (C_f), here estimated using the method of Peterson and Ryan (1986):

1-hr fuels:

$$\begin{aligned} if\ \frac{m_f}{m_{ext}} \leq 0.18, &\quad C_f = 1.0 \\ if\ 0.18 < \frac{m_f}{m_{ext}} \leq 0.73, &\quad C_f = 1.2 - 0.62\frac{m_f}{m_{ext}} \\ if\ \frac{m_f}{m_{ext}} > 0.73, &\quad C_f = 2.45 - 2.45\frac{m_f}{m_{ext}} \end{aligned} \quad (19)$$

10-hr fuels:

$$\begin{aligned} if\ \frac{m_f}{m_{ext}} \leq 0.12, &\quad C_f = 1.0 \\ if\ 0.12 < \frac{m_f}{m_{ext}} \leq 0.51, &\quad C_f = 1.09 - 0.72\frac{m_f}{m_{ext}} \\ if\ \frac{m_f}{m_{ext}} > 0.51, &\quad C_f = 1.47 - 1.47\frac{m_f}{m_{ext}} \end{aligned} \quad (20)$$

100-hr fuels:

$$\begin{aligned} if\ 0\frac{m_f}{m_{ext}} \leq 0.38, &\quad C_f = 0.98 - 0.85\frac{m_f}{m_{ext}} \\ if\ \frac{m_f}{m_{ext}} > 0.38, &\quad C_f = 1.06 - 1.06\frac{m_f}{m_{ext}} \end{aligned} \quad (21)$$

Where m_f = moisture content of fuel (dimensionless) and m_{ext} = fuel moisture of fire extinction (dimensionless). Fuels are split into three size classes: *1-hour* - <0.64cm, *10-hour* – 0.64-2.5cm, *100-hour* – 2.5cm-7.5cm, which each have characteristic surface are to volume ratio and drying rates. The 1-hr fuel class is split into live (green grass) and dead (dry grass, litter) classes, which have distinct behaviours. The input of each fuel class to the overall rate of spread is calculated by weighting the different fuel classes by their surface area to volume ratios.

The Rothermel model requires a number of inputs to predict fire intensity, summarised in Table 4. These have been selected from a combination of field measurements and standardised parameters from the literature. In addition to fixed fuel parameters, a number of inputs will be expected to change seasonally, namely fuel curing, fuel moisture and windspeed. These drivers are estimated as follows:

Fuel Curing: Annual curing (drying) of grass fuels is one of the key influences on annual fire intensity variation in miombo woodlands (Hoffa et al., 1999). The proportion of grass that is cured is approximated using NDVI measurements from MODIS, covering areas of Kilwa within the 5-35 tC/ha biomass range. As the relationship between NDVI and fuel curing is often inconsistent between locations, a 'relative greenness' value is calculated based on the maximum and minimum recorded NDVI value in each pixel (j):

$$RG_{i,j} = \frac{NDVI_{i,j} - NDVI_{min,j}}{NDVI_{max,j} - NDVI_{min,j}} \quad (22)$$

where i is the time of measurement and $NDVI_{max,j}$ and $NDVI_{min,j}$ are the maximum and minimum NDVI values recorded at each pixel over a specified time period. This time period was set to 3 years to maximise the chances of capturing extremes of NDVI whilst minimising the impact of land cover changes on the predictions of fuel curing (Newnham et al., 2011). This method is similar to that used in Australia's Grassland Fire Index and the United States National Fire Danger Rating System (NFDRS) (Burgan et al., 1998).

Fuel Moisture: Fuel moisture of dead fuel varies through the year based on rainfall events and subsequent drying. Dead fuel moisture is estimated using the method of Thonicke et al. (2010), which is based upon calculation of the Nesterov Index of fire danger (Nesterov, 1949):

$$NI(d) = \sum T_{max}(d) \cdot (T_{max}(d) - T_{dew}(d)) \quad (23)$$

where $T_{max}(d)$ is the maximum temperature and $T_{dew}(d)$ is the dew point at day d and summation is over the number of consecutive days that precipitation remains <3mm. When a day receives >3mm precipitation, the Nestrov Index resets to 0. Temperature and precipitation data are taken from the ERA-interim climate reanalysis dataset, and $T_{dew}(d)$ is approximated as $T_{min}(d) - 4$ (Running et al., 1987) where T_{min} is the minimum daily temperature. Moisture content for each fuel class is calculated as:

$$\omega_i = e^{-\alpha_i \cdot NI(d)} \quad (24)$$

where ω_i = relative fuel moisture of size class i, and α_i is applied to the three fuel classes in inverse proportion to the surface area to volume ratios ($\alpha_{1h} = 1.0 \cdot 10^{-3}$, $\alpha_{10h} = 5.42 \cdot 10^{-5}$, $\alpha_{100h} = 1.49 \cdot 10^{-5}$). Live fuel moisture is estimated from degree of curing, where a maximum greenness related to 230% moisture content, and minimum curing to 30% moisture content, where live fuels behave in the same manner as dead fuels. As a dynamic fuel model, fuel is transferred from the live to the dead class in proportion to the quantity of the grass fuel that is cured (Scott and Burgan, 2005).

Wind Speed: Wind has a considerable impact on fire behaviour, with stronger winds relating to a more intense fire. Wind speed at 10m is used from the ERA-interim dataset, and adjusted by a factor of 0.45 to represent the reduction of wind speed within woodlands.

Table 4 – Rothermel model parameters. Response variables are median early/late fire intensity. Model sensitivity is defined as $S_x = ([R_{adj} - R_n]/ R_n) / ([P_{adj} - P_n]/ P_n)$, where x is the factor by which the nominal value is changed, R_{adj} is the response for the model run with the adjusted value, R_n is the response with the nominal value, and P_n and P*adj* are the parameter values for the nominal and adjusted cases respectively.

			Early				Late				
Parameter Description	**Parameter Name**	**Nominal Value**	**$S_{0.5}$**	**$S_{0.75}$**	**$S_{1.5}$**	**S_2**	**$S_{0.5}$**	**$S_{0.75}$**	**$S_{1.5}$**	**S_2**	**Source**
Fuel mass (kg m^{-2})											
• grass	W_{live}	0.59	0.8	0.7	0.9	0.8	1.0	1.0	1.0	1.0	Field measurements (Kilwa).
• 1hr (other)	$W_{1\text{-}hr}$	0.11	0.1	0.1	0.2	0.2	0.0	0.0	0.0	0.1	
• 10hr	$W_{10\text{-}hr}$	0.05	0.0	0.0	0.0	0.0	0.0	0.0	0.0	0.0	
• 100hr	$W_{100\text{-}hr}$	0.06	-0.1	-0.1	-0.1	-0.1	0.0	0.0	-0.1	0.0	
Surface area to volume ratio (cm^{-1})											
• grass	σ_{live}	59.74	0.2	0.2	0.5	0.5	0.5	0.5	0.3	0.7	Field measurements (Nhambita). (σ_{live}, $\sigma_{1\text{-}hr}$)
• 1hr (other)	$\sigma_{1\text{-}hr}$	65.5	0.1	0.2	0.3	0.3	0.0	0.1	0.1	0.2	
• 10hr	$\sigma_{10\text{-}hr}$	3.58	0.0	0.0	0.0	0.0	0.0	0.0	0.0	0.0	(Scott and Burgan, 2005) ($\sigma_{10\text{-}hr}$, $\sigma_{100\text{-}hr}$)
• 100hr	$\sigma_{100\text{-}hr}$	0.98	0.0	0.0	0.0	0.0	0.0	0.0	0.0	0.0	
Fuelbed depth (m)	δ	0.45	1.0	1.0	1.0	1.0	1.1	1.1	1.1	1.1	Field measurements (Kilwa)
Wind adjustment factor	w_{adj}	0.45	1.1	1.2	1.4	1.5	1.2	1.3	1.5	1.6	Estimated, similar to Thonicke et al. (2010)
Max living fuel moisture	ω_{max}	120%	-0.9	-0.9	-0.5	-0.3	-0.3	-0.3	-0.2	-0.2	Scott and Burgan 2005)
Min living fuel moisture	ω_{min}	30%	-0.1	-0.1	-0.1	-0.1	-0.1	-0.1	-0.1	-0.1	Scott and Burgan 2005)
Fuel heat content (kJ kg^{-1})	h	18,622	1.5	1.7	2.4	2.7	1.5	1.7	2.5	3.0	Scott and Burgan 2005)
Fuel particle density (kg m^{-3})	ρ_p	513	0.1	0.1	0.0	0.0	0.1	0.1	0.0	0.0	Scott and Burgan 2005)
Minimum fireline intensity for continued combustion (kW/m)	I_{min}	50	0.0	0.0	0.0	0.0	0.0	0.0	0.0	0.0	Estimated

By running the model on a daily time step for all years of available data (2000-2012), a clear fire season is predicted beginning in mid-May, lasting through to December (Figure 12). Fire intensity is predicted to remain low in May/June, peak in September and reduce towards the end of the year. The model suggests that fire intensity is highly variable at any given time of year, though average intensity of late season fires are significantly greater than early season fires. By splitting these predicted fire intensities into 'early' (day ≤180) and 'late' (day>180) season fires, two different fire intensity PDFs were produced (Figure 6).

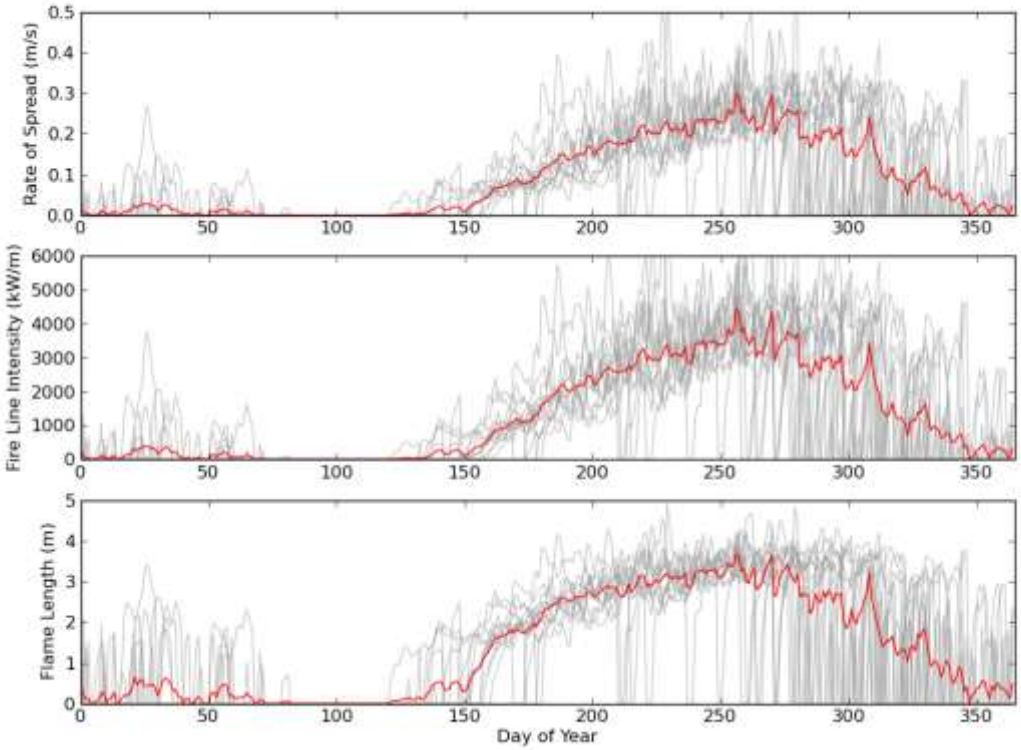

Figure 12 – Predictions of fire seasonality from the Rothermel model. Individual years (2000-2012) are plotted in grey and the mean of all years plotted in red.

References

Alexander, M. E. 1982. Calculating and interpreting forest fire intensities. *Canadian Journal of Botany,* 60**,** 349-357.

Bond, W. J. & Midgley, J. J. 2001. Ecology of sprouting in woody plants: the persistence niche. *Trends in Ecology & Evolution,* 16**,** 45-51.

Burgan, R. E., Klaver, R. W. & Klaver, J. M. 1998. Fuel models and fire potential from satellite and surface observations. *International Journal of Wildland Fire,* 8**,** 159-170.

Byram, G. 1959. Combustion of forest fuels. In 'Forest fire: control and use'.(Ed. KP Davis) pp. 61–89. McGraw-Hill: New York.

Campbell, B. M. 1996. *The Miombo in transition: woodlands and welfare in Africa*, Cifor.

Castellanos, J., Jaramilllo, V. C. J., Sanford JR, R. L. & Kauffman, J. B. 2001. Slash-and-burn effects on fine root biomass and productivity in a tropical dry forest ecosystem in Mexico. *Forest Ecology and Management,* 148**,** 41-50.

Chidumayo, E. N. 1997. *Miombo ecology and management: an introduction*, Intermediate Technology Publications Ltd (ITP).

Chidumayo, E. N. 2004. Development of Brachystegia-Julbernardia woodland after clear-felling in central Zambia: Evidence for high resilience. *Applied Vegetation Science,* 7**,** 237-242.

Desanker, P. V. 1996. Development of a MIOMBO woodland dynamics model in Zambezian Africa using Malawi as a case study. *Climatic Change,* 34**,** 279-288.

Desanker, P. V. & Prentice, I. C. 1994. MIOMBO – A vegetation dynamics model for the miombo woodlands of Zambezian Africa. *Forest Ecology and Management,* 69**,** 87-95.

Goldammer, J. G. & De Ronde, C. 2004. *Wildland fire management handbook for Sub-Sahara Africa*, African Minds.

Govender, N., Trollope, W. S. & Van Wilgen, B. W. 2006. The effect of fire season, fire frequency, rainfall and management on fire intensity in savanna vegetation in South Africa. *Journal of Applied Ecology,* 43**,** 748-758.

Hély, C., Alleaume, S., SwaP, R. & Justice, C. 2003. SAFARI-2000 characterization of fuels, fire behavior, combustion completeness, and emissions from experimental burns in infertile grass savannas in western Zambia. *Journal of Arid Environments,* 54**,** 381-394.

Hendricks, J. J., Hendrick, R. L., Wilson, C. A., Mitchell, R. J., Pecot, S. D. & Guo, D. 2006. Assessing the patterns and controls of fine root dynamics: an empirical test and methodological review. *Journal of Ecology,* 94**,** 40-57.

Hoffa, E. A., Ward, D., Hao, W., Susott, R. & Wakimoto, R. 1999. Seasonality of carbon emissions from biomass burning in a Zambian savanna. *Journal of Geophysical Research: Atmospheres,* 104**,** 13841-13853.

Jackson, J. F., Adams, D. C. & Jackson, U. B. 1999. Allometry of constitutive defense: A model and a comparative test with tree bark and fire regime. *American Naturalist,* 153**,** 614-632.

Johnson, E. A. & Miyanishi, K. 2001. *Forest fires: behavior and ecological effects*, Academic Press San Diego, CA.

Jones, H. G. 1992. *Plants and microclimate: a quantitative approach to environmental plant physiology*, Cambridge University Press.

Miller, C. & Urban, D. L. 2000. Modeling the effects of fire management alternatives on Sierra Nevada mixed-conifer forests. *Ecological Applications,* 10**,** 85-94.

Mlambo, D. & Mapaure, I. 2006. Post-fire resprouting of Colophospermum mopane saplings in a southern African savanna. *Journal of Tropical Ecology,* 22**,** 231-234.

Nesterov, V. 1949. Combustibility of the forest and methods for its determination. *Moscow: Goslesbumaga*.

Newnham, G. J., Verbesselt, J., Grant, I. F. & Anderson, S. A. 2011. Relative greenness index for assessing curing of grassland fuel. *Remote Sensing of Environment,* 115**,** 1456-1463.

Norman, J. M. & Campbell, G. S. 1991. Canopy structure. *Plant physiological ecology.* Springer.

Nottingham, A. 2004. *The characterisation of foliar N-concentrations and presence of N-fixers in Miombo woodland, Mozambique.* MRes, University of Dundee.

Peterson, D. L. & Ryan, K. C. 1986. Modeling postfire conifer mortality for long-range planning. *Environmental Management,* 10**,** 797-808.

Pyne, S. J., Andrews, P. L. & Laven, R. D. 1996. *Introduction to wildland fire*, John Wiley and Sons.

Robertson, F. E. 1993. Early-burning in the Brachystegia woodland of the Parks and Wild Life Estate. *Zimbabwe Science News,* 27**,** 68-71.

Rothermel, R. C. 1972. *A mathematical model for predicting fire spread in wildland fuels*, USFS.

Running, S. W., Nemani, R. R. & Hungerford, R. D. 1987. Extrapolation of synoptic meteorological data in mountainous terrain and its use for simulating forest evapotranspiration and photosynthesis. *Canadian Journal of Forest Research,* 17**,** 472-483.

Ryan, C. M. & Williams, M. 2011. How does fire intensity and frequency affect miombo woodland tree populations and biomass? *Ecological Applications,* 21**,** 48-60.

Ryan, C. M., Williams, M. & Grace, J. 2011. Above-and Belowground Carbon Stocks in a Miombo Woodland Landscape of Mozambique. *Biotropica,* 43**,** 423-432.

Saito, M., Poulter, B., Bellassen, V., Yue, C., Ryan, C. M., Williams, M., Luysseart, S., Ciais, P. & Peylin, P. *in prep*. Fire regimes and variability in above ground woody biomass in an African savanna woodland.

Scott, J. H. & Burgan, R. E. 2005. Standard fire behavior fuel models: a comprehensive set for use with Rothermel's surface fire spread model. *The Bark Beetles, Fuels, and Fire Bibliography***,** 66.

Shea, R. W., Shea, B. W., Kauffman, J. B., Ward, D. E., Haskins, C. I. & Scholes, M. C. 1996. Fuel biomass and combustion factors associated with fires in savanna ecosystems of South Africa and Zambia. *Journal of Geophysical Research: Atmospheres,* 101**,** 23551-23568.

Shugart, H. H. & Smith, T. M. 1996. A review of forest patch models and their application to global change research. *Climatic Change,* 34**,** 131-153.

Stocks, B., Van Wilgen, B., Trollope, W., Mcrae, D., Mason, J., Weirich, F. & Potgieter, A. 1996. Fuels and fire behavior dynamics on large-scale savanna fires in Kruger National Park, South Africa. *Journal of Geophysical Research,* 101**,** 23541-23,550.

Sutherland, E. K. & Smith, K. T. 2000. Resistance is not futile: the response of hardwoods to fire-caused wounding. *In:* Proceedings: workshop on fire, people, and the central hardwood landscape. General Technical Report NE-274, US Department of Agriculture, Forest Service, Northeastern Forest Experiment Station, Newtown Square, PA, 2000. 111-115.

Thonicke, K., Spessa, A., Prentice, I., Harrison, S., Dong, L. & Carmona-Moreno, C. 2010. The influence of vegetation, fire spread and fire behaviour on biomass burning and trace gas emissions: results from a process-based model. *Biogeosciences,* 7**,** 1991-2011.

Trollope, W., Trollope, L., Potgieter, A. & Zambatis, N. 1996. SAFARI-92 characterization of biomass and fire behavior in the small experimental burns in the Kruger National Park. *Journal of Geophysical Research,* 101**,** 23531-23,539.

Tuohy, J. & Choinski, J. 1990. Comparative photosynthesis in developing leaves of Brachystegia spiciformis Benth. *Journal of Experimental Botany,* 41**,** 919-923.

Tuohy, J. M., Prior, J. A. & Stewart, G. R. 1991. Photosynthesis in relation to leaf nitrogen and phosphorus content in Zimbabwean trees. *Oecologia,* 88**,** 378-382.

Waring, R., Landsberg, J. & Williams, M. 1998. Net primary production of forests: a constant fraction of gross primary production? *Tree Physiology,* 18**,** 129-134.

Williams, M. 1996. A three-dimensional model of forest development and competition. *Ecological Modelling,* 89**,** 73-98.

Woollen, E. 2013. *Carbon dynamics in African miombo woodlands: from the leaf to the landscape.* PhD, Edinburgh University.

Design credits: Figure 1, Horhew & redheadstock (deviantART.com).